Improved Isotherm Data for Adsorption of Methane on Activated Carbons

Wai Soong Loh,[†] Kazi Afzalur Rahman,[†] Anutosh Chakraborty,[‡] Bidyut Baran Saha,*[,§] Yoo Sang Choo,[||] Boo Cheong Khoo,[||] and Kim Choon Ng*[,†]

Department of Mechanical Engineering, National University of Singapore, 9 Engineering Drive 1, Singapore 117576, School of Mechanical and Aerospace Engineering, Nanyang Technological University, 50 Nanyang Avenue, Singapore 639798, Department of Mechanical Engineering, Kyushu University, 744 Motooka, Nishi-ku, Fukuoka-shi, Fukuoka 819-0395, Japan, and Department of Civil Engineering, National University of Singapore, 1 Engineering Drive 2, Singapore 117576

This article presents the adsorption isotherms of methane onto two different types of activated carbons, namely, Maxsorb III and ACF (A-20) at temperatures from (5 to 75) °C and pressures up to 2.5 MPa. The volumetric technique has been employed to measure the adsorption isotherms. The experimental results presented herein demonstrate the improved accuracy of the uptake values compared with previous measurement techniques for similar adsorbate−adsorbent combinations. The results are analyzed with various adsorption isotherm models. The heat of adsorption, which is concentration and temperature dependent, has been calculated from the measured isotherm data. Henry's law coefficients for these adsorbent−methane pairs are also evaluated at various temperatures.

Introduction

In recent years, adsorbed natural gas (ANG) has attracted much attention as a possible alternative to compressed natural gas (CNG) for energy storage and transportation purposes because the former can be designed to have a high-energy density but operates at a much lower pressure than the CNG method. The ANG storage system requires a porous adsorbent of high specific surface area to capture methane (CH_4) at room temperature,[1−3] and hitherto, the most promising adsorbents for natural gas (NG storage) are the microporous activated carbons with relatively high packing densities[4−6] and higher specific surface area[7] such as the pitch-based activated carbons (PACs) and activated carbon fibres (ACFs). These PACs and ACFs are versatile adsorbents because of their high surface area and micropore volumes where their bidisperse pore size distributions provide easy accessibility of molecules to the interior[8] and a relatively high thermal conductivity for improved thermal management.[9] For example, Maxsorb-III is developed from petroleum coke and blended with KOH at 400 °C for dehydration. It is chemically activated at (600 to 900) °C in an inert atmosphere for a greater surface area as well as a larger pore volume.[10] Similarly, the high carbon content activated carbon fiber (ACF), namely, A-20, is one of the best AC fibers that has similarly high pore volumes and surface areas when compared to the other activated carbon fibers (Pan, Polyacrylonitrile, Cellulose, etc.).[11]

In designing ANG storage, the adsorption characteristics of the adsorbate−adsorbent pair are the key information for vapor uptake capacity as well as the isosteric heat of adsorption. For this purpose, experimental adsorption isotherm data are measured for Maxsorb III and ACF (A-20) using a volumetric method. The temperature for such experiments ranges from (5 to 75) °C, while the pressures in the storage vessel are from atmospheric to 2.5 MPa. In the literature, some uptake data for the methane/Maxsorb III pair have been reported,[12,13] but the motivation of the present study is to gain better accuracy using a modified volumetric measurement technique rather than the reported desorption methods by Saha et al.[12] as opposed to Himeno et al.;[13] the temperature of the adsorbents is to be measured in this study and not implied through the bath temperatures. We intend to compare the experimental results of the ACF−methane system with the works of Lozano-Castelló et al.[11] where the samples were carried out in a high-pressure microbalance but at 25 °C. With a wider range of temperatures, the isotherm data are analyzed with the Langmuir, Tóth, and Dubinin-Astakhov (DA) adsorption isotherm equations. In addition, the isosteric heat of adsorption is studied not only with the Clausius−Clayperon equation; we introduce a correction term to account for the nonideality of the gaseous phase.[14] From the Tóth and Langmuir model, Henry's law coefficients for various temperatures are determined, and they are useful in assessing (i) the low uptake limit behavior of sorption gas at pressure $P \rightarrow 0$, (ii) the stability of adsorption isotherm models, and (iii) the maximum enthalpy of adsorption.

Experimental Section

The ultra pure methane sample supplied by SOXAL (Singapore Oxygen Air Liquid Pte Ltd., the purity grade 99.9995 %) was used for the present experiment. All properties of methane used in this paper were evaluated using the generalized equation of state proposed by Setzmann and Wagner.[15] The Maxsorb III sample, supplied by Kansai Coke and Chemicals Co. Ltd., Osaka, Japan, was in powder form, which is highly microporous, and the ACF (A-20) sample, supplied by Osaka Gas Co. Ltd., Japan, was of a fibrous type.

Measurement of Adsorbent Properties. The porous properties such as the BET surface area, the pore size, the pore volume, the porosity, and the skeletal density are listed in Table 1. These thermophysical properties were measured with an Autosorb

* Corresponding authors. Professor Kim Choon Ng. Phone: +65 65162214. E-mail: mpengkc@nus.edu.sg. Professor Bidyut Baran Saha. Phone: +81-92-8023101. E-mail: saha@mech.kyushu-u.ac.jp.
[†] Department of Mechanical Engineering, National University of Singapore.
[‡] Nanyang Technological University.
[§] Kyushu University.
[||] Department of Civil Engineering, National University of Singapore.

10.1021/je901011c
Published on Web 06/15/2010

Table 1. Thermophysical Properties of Maxsorb III and ACF A-20

adsorbent	surface area [$m^2 \cdot kg^{-1}$]	total pore volume [$m^3 \cdot kg^{-1}$]	average pore diameter [Å]	skeleton density [$kg \cdot m^{-3}$]	refs
Maxsorb III	$3.140 \cdot 10^6$	$20.1 \cdot 10^{-4}$	20.08	2200	9
ACF (A-20)	$2.206 \cdot 10^6$	$10.1 \cdot 10^{-4}$	21.611	2200	11

(Quantachrome gas sorption instrument) machine. The surface area was calculated by the Brunauer−Emmett−Teller (BET) method from the N_2 adsorption isotherm data, which has been performed at 77.3 K. The pore size distribution (PSD) of activated carbon fiber and activated carbon (type Maxsorb III) has been obtained by the nonlocal density functional theory (NLDFT) method.[16,17] The skeletal densities of these samples were measured by the automated Micromeritics AccuPyc 1330 pycnometer at room temperature. The pore size distribution (PSD) values for Maxsorb III and activated carbon fibers (ACF-A20) were calculated on the basis of N_2 adsorption data. To obtain a more realistic PSD appearance, the NLDFT reports (pore volume, $cm^3 \cdot g^{-1}$) have been derived by normalizing the pore volume to the pore size interval (differential volume dV/dr $cm^3 \cdot g^{-1} \cdot Å^{-1}$), and the PSD results are shown in Figure 1. It is observed that the NLDFT method exhibits few peaks on the PSD curves at a pore radius of 0.19 Å for Maxsorb III in the nanopore region of 4 Å. In the case of ACF, a peak is found at the pore radius of 0.15 Å in the nanopore region ranging from (4 to 10) Å. Therefore, it can be said that both the Maxsorb III and ACF A20 are highly microporous. It should be noted here that Figure 1 also provides the scanning electron microscope (SEM) photographs of Maxsorb III and ACF (A-20). The surface structure is observed to be flake-like layers with porous volumes entrenched in between in the case of Maxsorb III and cylindrical shapes with uniform surface diameter for ACF (A-20).

Measurement of Adsorption Isotherms. Figure 2 shows a schematic diagram of the experimental apparatus which mainly consists of a stainless steel (SS 304) adsorption cell and a charging cell with internal volume of (62.78 ± 1) mL and (1026.15 ± 1) mL, respectively. The samples were weighed by Computrac Max 5000 Moisture Analyzer with an uncertainty of ± 0.1 mg. The weights of the samples packed into the adsorption cell were (12.1715 and 5.1050) g, respectively, for

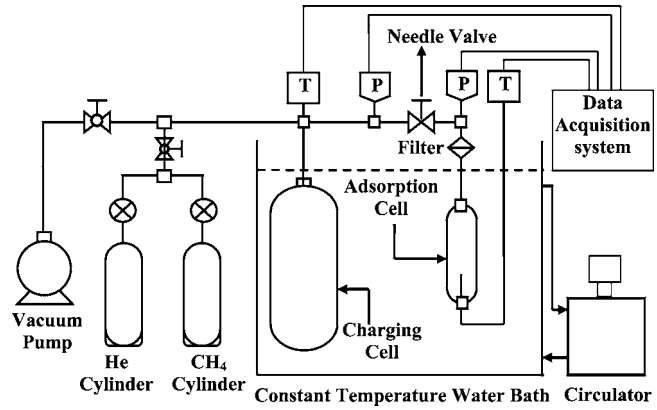

Figure 2. Schematic diagram of the experimental setup.

Maxsorb III and ACF (A-20). The adsorption cell was then connected to the charging cell through 1/4" nominal stainless steel plumbing and a set of Swagelok fittings (valves, T's, and reducers). Both the adsorption and charging cells were immersed in a constant-temperature water bath. The pressure readings of methane were measured using a (0 to 5) MPa range Kyowa pressure transducer (PGS-50KA) with an uncertainty of ± 0.1 % of full scale in measurement. The temperatures were recorded using class-A Pt 100 Ω RTDs with an estimated uncertainty of ± 0.15 K. The adsorption cell RTD was in contact with the activated carbon to enable the direct temperature measurement. Hence, the adsorption cell temperature is used as the isotherm temperature. All the temperatures and pressure readings are logged into an Agilent data logger to enable real time monitoring of the system. Owing to the continuous circulation of the bath fluid, and an adequate time for thermal stabilization, it is assumed that no temperature gradient would occur within the cells.

As the methane vapor is in a supercritical condition for the present measurement ranges, the experimental procedure is somewhat different from Loh et al.[18] where the adsorption characteristics of the activated carbon/HFC-134a pair were measured. Before commencing the experiment, the entire assembly was evacuated for 24 h to a vacuum level of 0.5 mbar, and a regeneration temperature of about (140 to 150) °C is maintained to enhance the removal of residue gas in

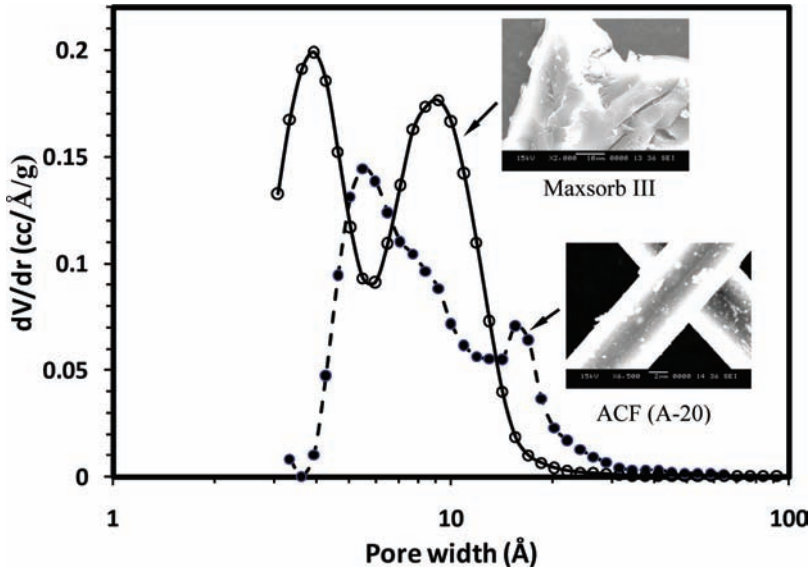

Figure 1. Pore size distributions of activated carbon (Maxsorb III) and activated carbon fiber (ACF-A20).

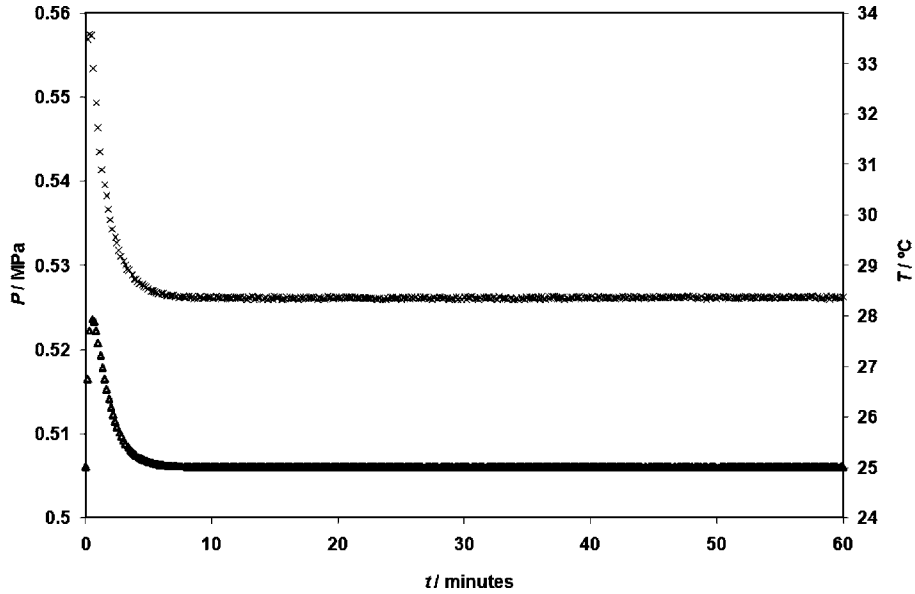

Figure 3. Typical pressure and temperature profiles for the methane/Maxsorb III pair during adsorption: ×, pressure (left ordinate); Δ, temperature (right ordinate).

the adsorbents. Pure helium gas is also purged into the system during regeneration to improve the evacuation. After evacuation, the charging cell is pressurized with methane vapor from its source with the needle valve being closed. The initial readings are recorded after the pressure and temperature are stabilized in the charging cell. The methane vapor is then released into the adsorption cell, and it took about an hour to reach the adsorption equilibrium state. Figure 3 shows the typical pressure and temperature profiles for the methane/Maxsorb III pair which indicates that the time interval was adequate to reach the equilibrium state during adsorption and was maintained for each data point for both of the samples. The adsorbed mass of methane was calculated from the amount of vapor transferred in the adsorption cell and the left over amount at the equilibrium state. Similarly, the charging cell is charged to the next higher pressure with the bath temperature remaining constant for the subsequent data point. Measurements were made up to 2.5 MPa, and the same procedures are repeated with different isotherms.

Data Reductions. The initially measured data are the pressure and temperature of both the adsorption cell and the charging cell. The mass of the methane is measured using the cell volumes and the density of the vapor for the corresponding pressure and temperature. The methane transferred to the adsorption cell ($m_{\text{adsorption\_cell}}$) is partly adsorbed in the micropores of the adsorbent and the left over vapor occupied in the void volume (V_{void}). Therefore, the adsorbed mass (m_{adsorbed}) is calculated from the following equation

$$m_{\text{adsorbed}} = m_{\text{adsorption\_cell}} - \rho_{\text{void}} V_{\text{void}} = m_{\text{adsorption\_cell}} - \rho_{\text{void}}\left(V_{\text{adsorption\_cell}} - \frac{m_{\text{ac}}}{\rho_{\text{solid}}} - v_{\mu} m_{\text{ac}}\right) \quad (1)$$

where ρ_{void} is the density of methane vapor as a function of pressure and temperature of the adsorption cell; $V_{\text{adsorption\_cell}}$ is the adsorption cell volume; m_{ac} is the mass of the activated carbon sample in the adsorption cell; ρ_{solid} is the solid density of the activated carbon; and v_{μ} is the micropore volume of the activated carbon. Hence, the amount of methane uptake is calculated as $C = m_{\text{adsorbed}}/m_{\text{ac}}$. The experimentally measured uptake data for adsorption of methane on Maxsorb III and ACF (A-20) are furnished in Tables 2 and 3, respectively. The overall uncertainty is found to be 4 % of the uptake amount for this experimental technique, which is typical using the volumetric method.[13]

Table 2. Experimental Uptake Data for Adsorption of Methane on Maxsorb III

P	C	P	C	P	C	P	C
MPa	kg·kg^{-1}	MPa	kg·kg^{-1}	MPa	kg·kg^{-1}	MPa	kg·kg^{-1}
T = 5 °C		T = 15 °C		T = 25 °C		T = 35 °C	
0.050	0.015	0.050	0.012	0.057	0.011	0.060	0.010
0.127	0.033	0.135	0.029	0.140	0.025	0.152	0.022
0.217	0.050	0.233	0.045	0.234	0.038	0.245	0.034
0.310	0.066	0.331	0.059	0.331	0.050	0.344	0.045
0.411	0.080	0.429	0.071	0.428	0.061	0.443	0.055
0.510	0.093	0.526	0.082	0.526	0.071	0.543	0.064
0.646	0.109	0.655	0.096	0.652	0.083	0.678	0.076
0.784	0.123	0.800	0.109	0.792	0.095	0.820	0.087
0.934	0.136	0.946	0.121	0.948	0.108	0.974	0.098
1.138	0.152	1.155	0.137	1.157	0.122	1.175	0.111
1.340	0.167	1.354	0.150	1.344	0.134	1.373	0.122
1.550	0.180	1.561	0.163	1.563	0.147	1.571	0.133
1.754	0.191	1.762	0.174	1.756	0.157	1.771	0.143
1.949	0.201	1.968	0.184	1.960	0.167	1.975	0.153
2.158	0.211	2.166	0.193	2.157	0.176	2.178	0.161
T = 45 °C		T = 55 °C		T = 65 °C		T = 75 °C	
0.061	0.008	0.065	0.008	0.067	0.007	0.071	0.006
0.148	0.019	0.160	0.017	0.157	0.015	0.162	0.013
0.248	0.029	0.255	0.026	0.254	0.023	0.263	0.020
0.348	0.039	0.354	0.035	0.350	0.030	0.362	0.027
0.445	0.048	0.458	0.043	0.456	0.038	0.464	0.034
0.540	0.056	0.555	0.050	0.555	0.045	0.561	0.040
0.665	0.065	0.680	0.059	0.681	0.053	0.686	0.047
0.815	0.076	0.823	0.069	0.826	0.061	0.835	0.055
0.966	0.086	0.974	0.078	0.978	0.070	0.987	0.063
1.170	0.099	1.204	0.091	1.188	0.081	1.198	0.073
1.368	0.110	1.389	0.100	1.393	0.091	1.401	0.083
1.585	0.121	1.593	0.110	1.589	0.100	1.603	0.091
1.777	0.130	1.799	0.120	1.795	0.108	1.806	0.099
1.975	0.139	1.984	0.127	1.990	0.116	2.015	0.107
		2.203	0.136	2.187	0.124	2.198	0.114

Three different models, those of Langmuir, Tóth, and Dubinin-Astakhov, have been used to correlate the experimental equilibrium uptake values. The Langmuir model is the simplest model which describes the monolayer type adsorption (Type I isotherm of the IUPAC classification) in

Table 3. Experimental Uptake Data for Adsorption of Methane on ACF (A-20)

P	C	P	C	P	C	P	C
MPa	kg·kg^{-1}	MPa	kg·kg^{-1}	MPa	kg·kg^{-1}	MPa	kg·kg^{-1}
T = 5 °C		T = 15 °C		T = 25 °C		T = 35 °C	
0.057	0.012	0.056	0.010	0.059	0.008	0.059	0.007
0.128	0.022	0.143	0.022	0.144	0.018	0.146	0.015
0.218	0.034	0.242	0.032	0.252	0.028	0.247	0.023
0.332	0.045	0.343	0.041	0.350	0.036	0.352	0.031
0.437	0.055	0.443	0.049	0.451	0.043	0.445	0.037
0.549	0.063	0.550	0.057	0.550	0.050	0.545	0.043
0.672	0.072	0.699	0.066	0.688	0.058	0.694	0.051
0.855	0.082	0.838	0.074	0.838	0.066	0.846	0.058
0.981	0.089	0.997	0.082	0.999	0.073	0.998	0.065
1.162	0.097	1.205	0.091	1.199	0.081	1.204	0.073
1.358	0.105	1.401	0.099	1.401	0.089	1.404	0.080
1.572	0.113	1.601	0.106	1.605	0.095	1.599	0.086
1.780	0.120	1.799	0.112	1.805	0.101	1.820	0.092
1.981	0.126	2.008	0.118	2.000	0.107	2.034	0.098
2.202	0.132	2.207	0.123	2.206	0.112	2.201	0.102
2.412	0.137	2.406	0.128	2.402	0.117	2.433	0.108
T = 45 °C		T = 55 °C		T = 65 °C		T = 75 °C	
0.062	0.006	0.051	0.004	0.067	0.004	0.059	0.003
0.157	0.014	0.157	0.012	0.147	0.009	0.151	0.008
0.261	0.021	0.254	0.018	0.249	0.015	0.249	0.013
0.354	0.027	0.360	0.024	0.358	0.020	0.346	0.017
0.452	0.032	0.453	0.029	0.457	0.025	0.445	0.021
0.561	0.038	0.562	0.034	0.551	0.029	0.544	0.025
0.694	0.044	0.711	0.041	0.702	0.035	0.723	0.032
0.845	0.051	0.854	0.047	0.861	0.041	0.850	0.037
1.001	0.057	1.005	0.053	1.009	0.047	1.027	0.042
1.206	0.065	1.200	0.059	1.203	0.053	1.198	0.048
1.414	0.072	1.407	0.066	1.403	0.059	1.403	0.053
1.602	0.078	1.609	0.072	1.599	0.064	1.603	0.058
1.804	0.083	1.803	0.077	1.833	0.070	1.825	0.064
2.038	0.090	1.995	0.082	2.005	0.074	2.001	0.068
2.230	0.094	2.198	0.087	2.236	0.080	2.199	0.072
2.394	0.098	2.416	0.091	2.403	0.083	2.402	0.075

microporous solids, such as adsorption of methane in activated carbon. The Langmuir model presumes a homogeneous surface of the adsorbents where the adsorption energy is constant over all sites. This model has also assumed that the adsorption on the surface is localized, and each site can accommodate only one molecule or atom.[19] The Langmuir model is written as

$$\frac{C}{C_0} = \frac{k_0 \exp(\Delta h_{st}/RT)P}{1 + k_0 \exp(\Delta h_{st}/RT)P} \tag{2}$$

where C_0 is the saturated amount adsorbed; P is the equilibrium pressure; k_0 is the equilibrium constant; Δh_{st} is the isosteric heat of adsorption; and R is the gas constant.

The Langmuir model has limitations to fit at high pressure and for material heterogeneity. The Tóth model is commonly used for heterogeneous adsorbents such as activated carbon because of its correct behavior at both the low and high pressure ends.[19] The Tóth model can be represented by

$$\frac{C}{C_0} = \frac{k_0 \exp(\Delta h_{st}/RT)P}{\{1 + (k_0 \exp(\Delta h_{st}/RT)P)^t\}^{1/t}} \tag{3}$$

where t is the parameter that indicates the heterogeneity of the adsorbent. The Tóth model is identical to the Langmuir model when the heterogeneity parameter (t) becomes unity.

Dubinin and Astakhov proposed the following model for adsorption of vapors and gases onto nonhomogeneous carbonaceous solids with a wide pore size distribution.[19] This D−A model allows for the surface heterogeneity and extends to high pressure.

$$W = W_0 \exp\left[-\left(\frac{A}{E}\right)^n\right] \tag{4}$$

where A is the adsorption potential and W is the amount of uptake in cm^3·g^{-1}; W_0 is the limiting uptake of adsorption space of the adsorbent in cm^3·g^{-1}; E is the characteristic energy of the adsorption system; and n is the structural heterogeneity parameter, which is typically varied from 1.2 to 1.8 for activated carbons.[19] The adsorption potential, A, is the specific work done in the isothermal compression of a unit mass of vapor from P to the saturation vapor pressure P_s and is given by

$$A = RT \ln\left(\frac{P_s}{P}\right) \tag{5}$$

Thus, eq 4 can be expressed as[20]

$$\frac{W}{W_0} = \exp\left[-\left\{\frac{RT}{E} \ln\left(\frac{P_s}{P}\right)\right\}^n\right] \tag{6}$$

As the methane vapor is in the supercritical state for the present experimental conditions, it is necessary to estimate the adsorbed phase volume and the saturated vapor pressure (P_s) to apply the D−A model. The adsorbed phase specific volume (v_a) is estimated using the following equation[12] in sequence with that used for high-pressure gases.[21]

$$v_a = v_b \exp[\alpha[T - T_b]] \tag{7}$$

where v_b is the specific volume of the liquid at the boiling point and T_b and α are the thermal expansion coefficient of the superheated liquid which was assumed as an average value of 0.0025 K^{-1}. The temperature dependence of α can also be expressed as follows from its definition of thermal expansion for liquids.

$$\alpha = \frac{1}{v_a}\left(\frac{\partial v_a}{\partial T}\right)_P \approx \frac{1}{T} \tag{8}$$

The pseudovapor pressure, P_s, at a given isotherm temperature is calculated by Dubinin's method[20] that has been used for methane in earlier studies.[12,13,22]

$$P_s = \left(\frac{T}{T_c}\right)^2 P_c \qquad (T > T_c) \tag{9}$$

where P_c and T_c are the critical pressure and the critical temperature of methane.

Results and Discussion

Adsorption Isotherms. Figures 4 and 5 show the adsorption isotherm data for methane uptake on Maxsorb III and ACF (A-20) at temperatures ranging from (5 to 75) °C and pressures up to 2.5 MPa. It is observed that the experimental uptake profiles are categorized to the Type I adsorption isotherm (monolayer coverage) of the IUPAC classification, and hence the Langmuir model has been considered to fit the experimental data. Again, the adsorbent samples used in this study are found to be highly microporous and heterogeneous in surface structure from their pore size distribution. As the Tóth model incorporates the surface heterogeneity of the adsorbent and is applicable for a wide pressure range, it is also appropriate to fit the experimental data. The regressed isotherms with both the Langmuir and Tóth models are shown

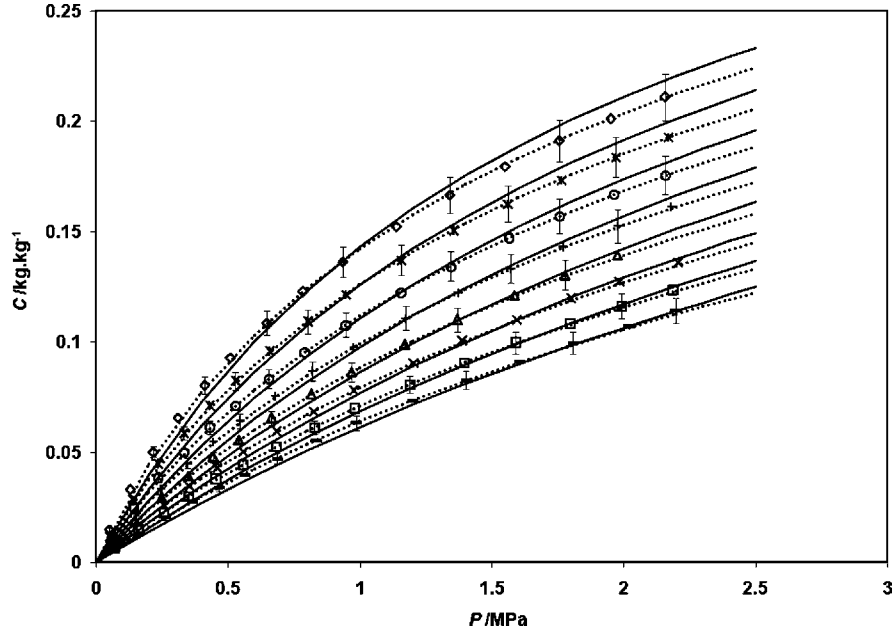

Figure 4. Adsorption isotherms of methane on Maxsorb III with error bars of 5 %: ◇, 5 °C; ∗, 15 °C; ○, 25 °C; +, 35 °C; Δ, 45 °C; ×, 55 °C; □, 65 °C; —, 75 °C; solid lines are from the Langmuir model, and broken lines are from the Tóth model.

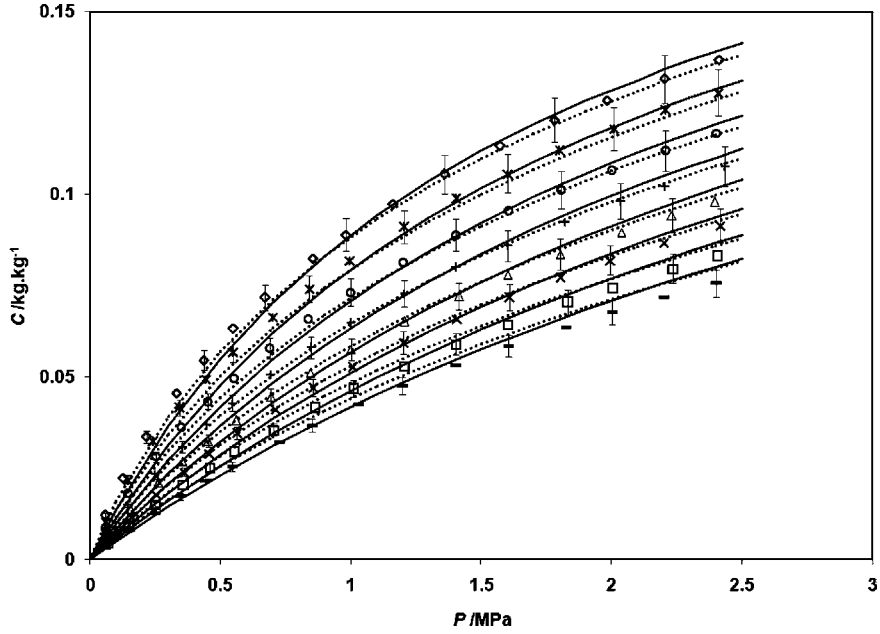

Figure 5. Adsorption isotherms of methane on ACF (A-20) with error bars of 5 %: ◇, 5 °C; ∗, 15 °C; ○, 25 °C; +, 35 °C; Δ, 45 °C; ×, 55 °C; □, 65 °C; —, 75 °C; solid lines are from the Langmuir model, and broken lines are from the Tóth model.

in Figure 4 for Maxsorb III and Figure 5 for ACF (A-20). The numerical value of the model parameters (C_0, k_0, Δh_{st}, and t) are listed in Table 4. The error of regression has also been calculated using the following equation to compare the isotherm model results with the experimental data.

$$\text{error of regression} = \frac{\sqrt{\frac{1}{N}\sum_{i=1}^{N}(C_{\text{expt}} - C_{\text{model}})^2}}{\frac{1}{N}\sum_{i=1}^{N} C_{\text{expt}}} \quad (10)$$

where N is the number of data points.

Table 4. Adsorption Parameters (C_0, k_0, Δh_{st}, and t) for the Langmuir and Tóth Models

	Maxsorb III		ACF (A-20)	
parameters	Langmuir	Tóth	Langmuir	Tóth
C_0 (g·g^{-1})	0.402	0.439	0.232	0.277
$\Delta h_{st}/R$ (K)	1550	1610	1440	1453.6
$k_0 \cdot 10^3$ (MPa^{-1})	2.10	1.97	3.50	3.65
t	1.0	0.780	1.0	0.742
error of regression (%)	4.2	1.0	4.4	2.6

The Tóth model provides a better fit than the Langmuir model to the experimental adsorption isotherms of methane for both of the adsorbents due to the account of the heterogeneity parameter (t). However, the Langmuir model is simpler than the Tóth model and also did not deviate much from the measured uptake values

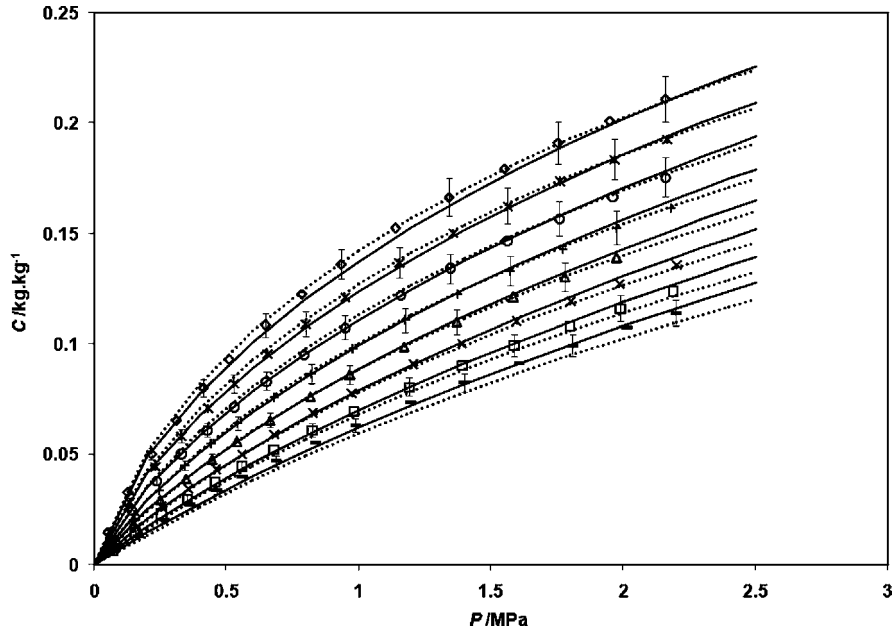

Figure 6. Adsorption isotherms of methane on Maxsorb III with error bars of 5 %: ◇, 5 °C; ∗, 15 °C; ○, 25 °C; +, 35 °C; Δ, 45 °C; ×, 55 °C; □, 65 °C; —, 75 °C; solid lines are from the D−A model fit ($\alpha = 1/T$), and broken lines are from the D−A model fit ($\alpha = 0.0025$).

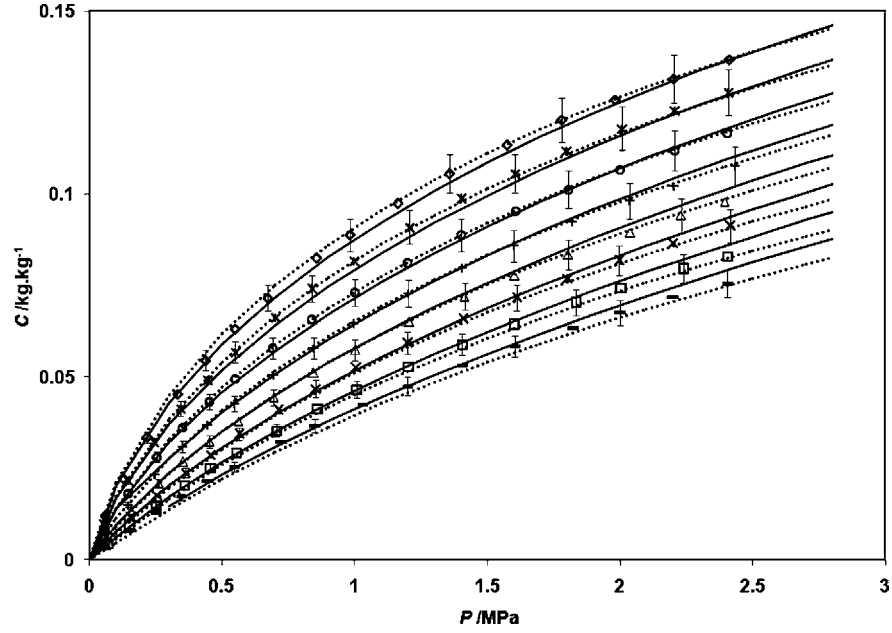

Figure 7. Adsorption isotherms of methane on ACF (A-20) with error bars of 5 %: ◇, 5 °C; ∗, 15 °C; ○, 25 °C; +, 35 °C; Δ, 45 °C; ×, 55 °C; □, 65 °C; —, 75 °C; solid lines are from the D−A model fit ($\alpha = 1/T$), and broken lines are from the D−A model fit ($\alpha = 0.0025$).

for the present pressure and temperature ranges. Since the adsorbed natural gas storage system operates at (2 to 4) MPa and at ambient temperature, either of these two models can be used in designing and simulation of the ANG storage system.

The Dubinin−Astakhov model is employed to fit the uptake data with adsorbed phase volume correction. Figures 6 and 7 represent the adsorption uptake data of methane on Maxsorb III and ACF (A-20), respectively, regressed with the D−A isotherm model. The average error of analysis is within ± 3 % for both the cases of $\alpha = 0.0025$ and $\alpha = 1/T$ which indicates the D−A model is also appropriate for the present adsorbate−adsorbent pairs, although the D−A model does not have a Henry's law regime. The adsorption parameters (W_0, E, and n) are listed in Table 5. It is found that the value of the maximum volumetric uptake (W_0) is higher in the case of $\alpha = 1/T$ than $\alpha = 0.0025$ for both of the adsorbents and consequently a lower value of characteristic energy (E) and heterogeneity parameter (t). This is because of the relatively higher value of the adsorbed phase specific volume (v_a) when the thermal expansion coefficient (α) is used as $1/T$ instead of 0.0025.

Table 5. Adsorption Parameters for the D−A Isotherm (W_0, E, and n) Modeled with Adsorbed Phase Volume Correction

	Maxsorb III		ACF (A-20)	
parameters	$\alpha/K^{-1} = 0.0025$	$1/T$	0.0025	$1/T$
$W_0/cm^3 \cdot g^{-1}$	1.211	1.618	0.717	0.941
$E/J \cdot mol^{-1}$	5835.1	5257.5	6198.4	5640.5
n	1.46	1.33	1.51	1.37
error of regression (%)	2.55	1.85	1.76	2.22

The equilibrium uptakes of methane on both adsorbents have been compared with data cited from the literature,[11−13] and these are shown in Figure 8. The predicted uptake values of Saha et

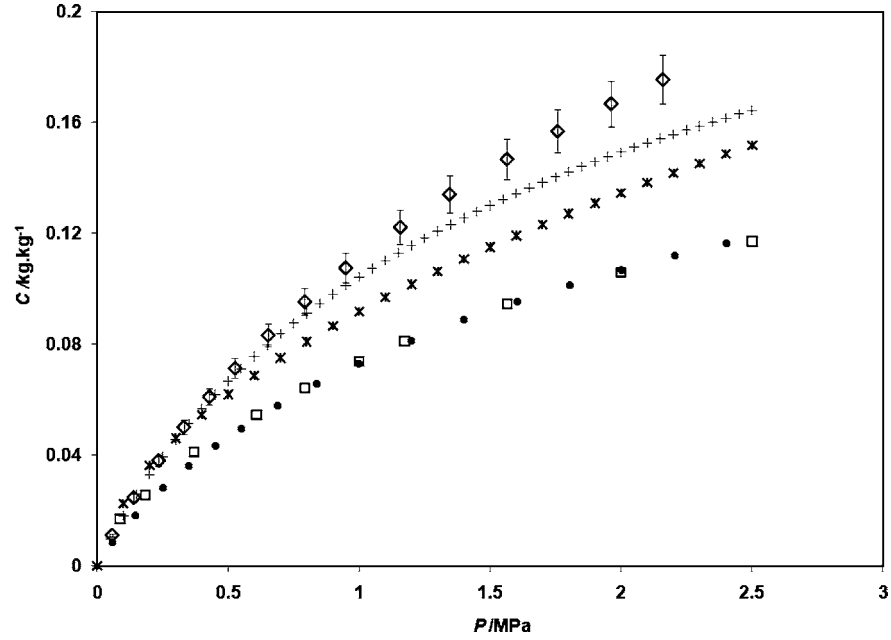

Figure 8. Comparison of adsorption isotherm data at 25 °C from the cited literature: ◇, present study on Maxsorb III (with 5 % error bars); +, Himeno et al.[12] on Maxsorb sample; ∗, Saha et al.[11] on Maxsorb III; ●, present study on ACF (A-20); □, Lozano-Castelló et al.[13] on ACF (A-20).

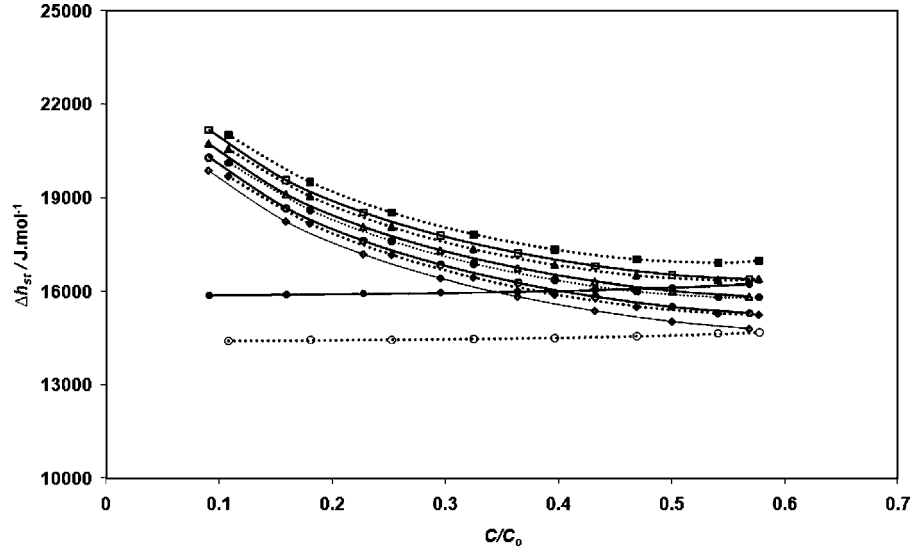

Figure 9. Uptake-dependent isosteric heat of adsorption calculated from the D−A model for Maxsorb III (solid symbols) and ACF (empty symbols): ◇/◆, 5 °C; ○/●, 25 °C; Δ/▲, 45 °C; □/■, 65 °C. Horizontal lines are from the Tóth isotherm model at 25 °C.

al.[12] are about (10 to 15) % lower than the present study because of their measurement technique and utilization of a different batch Maxsorb III in which the BET surface area was about 5 % lower than that of the present Maxsorb III. Saha et al.[12] have regressed the adsorption parameters from the differential uptake between two equilibrium adsorption states instead of absolute uptake for the corresponding equilibrium states which underpredicts the experimental results. Furthermore, Himeno et al.[13] have measured the uptake values of methane onto a Maxsorb sample with the volumetric technique which are (8 to 10) % lower than the present adsorption uptake data. The porous properties of the Maxsorb sample used in the study of Himeno et al.[13] are comparable but slightly lower than Maxsorb III. Another reason for deviation observed between the present uptake data and the data obtained by Himeno et al.[13] could be the taking of the bath temperature as the isotherm temperature, whereas the adsorbent temperature is considered as the isotherm temperature in the present study. Nevertheless, the present experimental data on ACF (A-20) are fairly matched (deviation below 3 %) with the isotherm at 25 °C for the same sample which has been carried out in a high-pressure microbalance by Lozano-Castelló et al.[11]

Isosteric Heat of Adsorption. Figure 9 shows the uptake-dependent heat of adsorption (Δh_{st}) at different isothermal conditions for both Maxsorb III and ACF (A-20). The values of the heat of adsorption (Δh_{st}) have been extracted from the isotherm data using the Clausius−Clayperon equation along with a correction term for the nonideality of the gaseous phase, recently derived by Chakrabarty et al.,[14] which is as follows.

$$\Delta h_{st} = RT^2\left[\left(\frac{\partial(\ln P)}{\partial T}\right)_C\right] + Tv_g\frac{dP}{dT}(P,T) \qquad (11)$$

Here, the first term of the right-hand side is derived from the Clausius−Clayperon equation and can be expanded by using the D−A isotherm model with $\alpha = 1/T$. A second term is introduced which defines the behavior of the adsorbed mass with respect to both the pressure and the temperature changes

Table 6. Henry's Law Coefficients, K_H/MPa^{-1}

T	calculated from Tóth model		calculated from Langmuir model	
°C	Maxsorb III	ACF (A-20)	Maxsorb III	ACF (A-20)
5	0.283	0.188	0.222	0.144
15	0.231	0.157	0.183	0.121
25	0.192	0.132	0.153	0.102
35	0.161	0.113	0.129	0.087
45	0.137	0.097	0.110	0.075
55	0.117	0.085	0.095	0.066
65	0.101	0.074	0.083	0.058
75	0.088	0.066	0.072	0.051

during an adsorbate uptake, which occurs due to the nonideality of the gaseous phase. Ultimately, eq 11 becomes

$$\Delta h_{st} = 2RT + E\left[\left(\ln\frac{W_0}{Cv_a}\right)^{1/n} + \frac{1}{n}\left(\ln\frac{W_0}{Cv_a}\right)^{1-n/n}\right] + Tv_g\frac{dP}{dT}(P,T) \quad (12)$$

where v_g is the specific volume of the vapor phase and dP/dT represents the gradient of the pressure with the temperature of the adsorbate.

It can be seen that the heat of adsorption (Δh_{st}) varies with the adsorbate surface loading which confirms the surface heterogeneity for both samples. Otherwise, the adsorption energy is constant over all sites if the surface is homogeneous.[19] As there is a change in energy level during the adsorption/desorption process, an effective cooling/heating arrangement is to be installed to enhance the charging/discharging rate of an adsorptive gas storage system.

The Δh_{st} values derived from the Tóth isotherm model are also represented in Figure 9. A slight increase of the Δh_{st} value along with the increase of surface loading (C/C_0) is due to the taking of nonideality of the gaseous phase as the gas properties are pressure and temperature dependent.

Henry's Law Coefficient. The Henry's region is the low pressure and low uptake regime, where each gas molecule can explore the whole adsorbent surface independently. As both the Langmuir and Tóth isotherm are valid at the low and high end of the pressure range, they do possess the correct Henry law type behavior.[19] So, the temperature-dependent Henry's law coefficients (K_H) can be determined using the following equation.

$$K_H = \frac{\partial C}{\partial P}_{P\to 0} = C_0 k_0 \exp\left(\frac{\Delta h_{st}}{RT}\right) \quad (13)$$

The coefficients for the assorted activated carbons at different temperatures are listed in Table 6. The K_H values decrease as the temperatures increase for both types of adsorbents which indicates the amount of gas adsorbed/desorbed is less at relatively higher temperatures but the isosteric heat is the largest in the Henry's region.

Conclusions

The adsorption characteristics are the basic parameters of any adsorbate−adsorbent system. In this study, experimental isotherms have been derived for two different activated carbons and methane systems which are useful for the charging and discharging analysis of natural gas storage systems. For the measured adsorption data, an improvement in accuracy has been observed in the present study compared to that of earlier methods. The Maxsorb III sample shows a higher storage capacity because of its high specific pore volume and surface area than the ACF (A-20) sample. The isosteric heat of adsorption is determined from the measured isotherm data which is useful in designing an effective cooling/heating arrangement for the adsorbed natural gas storage system. The temperature-dependent Henry's law coefficients are also helpful in assessing the low uptake limit behavior of the storage systems.

Literature Cited

(1) Lozano, D.; De la Casa, M. A.; Alcãniz, J.; Cazorla, D.; Linares, A. Advances in the study of methane storage in porous carbonaceous materials. *Fuel* **2002**, *81*, 1777–1803.

(2) Menon, V. C.; Komarneni, S. Porous Adsorbents for Vehicular Natural Gas Storage: A Review. *J. Porous Mater.* **1998**, *5*, 43–58.

(3) Chakraborty, A.; Saha, B. B.; Ng, K. C.; Koyama, S.; Srinivasan, K. Theoretical Insight of Physical Adsorption for a Single-Component Adsorbent + Adsorbate System: I. Thermodynamic Property Surfaces. *Langmuir* **2009**, *25* (4), 2204–2211.

(4) Esteves, I. A. A. C.; Lopes, M. S. S.; Nunes, P. M. C.; Mota, J. P. B. Adsorption of natural gas and biogas components on activated carbon. *Sep. Purif. Technol.* **2008**, *62*, 281–296.

(5) Alcãz-monge, J.; Lozano-Castelló, D.; Cazorla-amórs, D.; Linares-solano, A. Fundamentals of methane adsorption in microporous carbons. *Microporous Mesoporous Mater.* **2009**, *124* (1−3), 110–116.

(6) Quinn, D. F.; Macdonald, J. A. Natural Gas Storage. *Carbon* **1992**, *30* (7), 1097–1103.

(7) Chakraborty, A.; Saha, B. B.; Ng, K. C.; Koyama, S.; Srinivasan, K. Theoretical Insight of Physical Adsorption for a Single-Component Adsorbent + Adsorbate System: II. The Henry Region. *Langmuir* **2009**, *25* (13), 7359–7367.

(8) Ruthven, D. M. *Principles of adsorption and adsorption processes*; John Wiley & Sons: New York, 1984.

(9) Saha, B. B.; Chakraborty, A.; Koyama, S.; Yoon, S. H.; Kumja, M.; Yap, C. R.; Ng, K. C. Isotherms and thermodynamics for the adsorption of n-butane on Maxsorb III. *Int. J. Heat Mass Transfer* **2008**, *51*, 1582–1589.

(10) Otowa, T.; Tanibata, T.; ltoh, M. Production and adsorption characteristics of MAXSORB: high-surface-area active carbon. *Gas Sep. Purif.* **1993**, *7* (4), 241–245.

(11) Lozano-Castelló, D.; Cazorla-Amorós, D.; Linares-Solano, A. Powdered Activated Carbons and Activated Carbon Fibers for Methane Storage: A Comparative Study. *Energy Fuels* **2002**, *16*, 1321–1328.

(12) Saha, B. B.; Koyama, S.; El-Sharkawy, I. I.; Habib, K.; Srinivasan, K.; Dutta, P. Evaluation of Adsorption Parameters and Heats of Adsorption through Desorption Measurements. *J. Chem. Eng. Data* **2007**, *52*, 2419–2424.

(13) Himeno, S.; Komatsu, T.; Fujita, S. High pressure adsorption equilibria of methane and carbon dioxide on several activated carbons. *J. Chem. Eng. Data* **2005**, *50*, 369–376.

(14) Chakraborty, A.; Saha, B. B.; Koyama, S.; Ng, K. C. On the thermodynamic modeling of the isosteric heat of adsorption and comparison with experiments. *Appl. Phys. Lett.* **2006**, *89*, 171901.

(15) Setzmann, U.; Wagner, W. A new equation of state and tables of thermodynamic properties for methane covering the range from the melting line to 625 K at pressures up to 1000 MPa. *J. Phys. Chem. Ref. Data* **1991**, *20* (6), 1061–1151.

(16) Jagiello, J.; Thommes, M. Comparison of DFT characterization methods based on N_2, Ar, CO_2, and H_2 adsorption applied to carbon with various pore size distributions. *Carbon* **2004**, *42*, 1227–1232.

(17) Rathouský, J.; Thommes, M. Adsorption properties and advanced textural characterization of novel micro/mesoporous zeolites. *Stud. Surf. Sci. Catal.* **2007**, *174* (2), 1042–1047.

(18) Loh, W. S.; Kumja, M.; Rahman, K. A.; Ng, K. C.; Saha, B. B.; Koyama, S.; El-Sharkawy, I. I. Adsorption parameter and heat of adsorption of activated carbon/HFC-134a pair. *Heat Transfer Eng.* **2010**, *31* (11), 910–916.

(19) Do, D. D. *Adsorption Analysis: Equilibria and Kinetics*; Imperial College Press: London, 1998.

(20) Dubinin, M. M. The potential theory of adsorption of gases and vapors for adsorbents with energetically nonuniform surfaces. *Chem. Rev.* **1960**, *60*, 1–70.

(21) Ozawa, S.; Kusumi, S.; Ogino, Y. Physical Adsorption of Gases at High Pressure. *J. Colloid Interface Sci.* **1976**, *56*, 83–91.

(22) Amankwah, K. A. G.; Schwarz, J. A. A modified approach for estimating pseudo vapor pressures in the application of the Dubinin-Astakhov equation. *Carbon* **1995**, *33*, 1313–1319.

Received for review November 29, 2009. Accepted May 29, 2010. The authors' gratefully acknowledge the financial support given by grants (R33-2009-000-1966-0) from World Class University (WCU), Project of the National Research Foundation, Korea, (R265-000-268-305) from A*STAR/MPA, Singapore, and (R265-000-286-597) from King Abdullah University of Science and Technology (KAUST), KSA.

JE901011C